AEA-RS-1232

BENCHMARK TESTING OF JEF2.2 DATA FOR SHIELDING APPLICATIONS:

ANALYSIS OF THE WINFRITH WATER BENCHMARK EXPERIMENT.

H.F.Locke (Mrs.) & G.A.Wright

Reactor Physics Shielding and Criticality Department
Safety Engineering Systems Division
AEA Reactor Services
Winfrith Tecnology Centre
Dorchester
Dorset DT2 8DH

February 1993

BENCHMARK TESTING OF JEF2.2 DATA FOR SHIELDING APPLICATIONS:

ANALYSIS OF THE WINFRITH WATER BENCHMARK EXPERIMENT.

H.F.Locke (Mrs.) & G.A.Wright

Reactor Physics Shielding and Criticality Department
Safety Engineering Systems Division
AEA Reactor Services

AEA Project Reference No. N.D.1

NSRMU Project Reference No. RPS/AGR/05

Summary

This report describes the analysis of the Winfrith water benchmark experiment using the Monte Carlo code MCBEND for the validation of JEF2.2 cross-section data. Results are presented for the high energy S32(n,p)P32 reaction rate and neutron spectra above 1MeV for a range of source-detector spacings. The MCBEND calculation gives a slight overprediction of the S32(n,p)P32 reaction rate, averaging about 12%.However there is no clear indication that this difference increases with penetration distance The calculated spectra are in good agreement over the range 1.7 to 8.8MeV with C/M in the range 0.8 to 1.3 and being generally within two standard deviations of unity.

These results indicate that JEF2.2 cross-section data for hydrogen and for oxygen is valid for use in Monte Carlo calculations using MCBEND for neutron energies in the range 1.7 to 8.8MeV.

February 1993

AEA-RS-1232

CONTENTS

TABLES

FIGURES

1. INTRODUCTION

The JEF2 nuclear data library (1) has now been released in the form of JEF2.2 for benchmark testing (2). For shielding applications the benchmarking in the UK is being performed in two stages. The first stage involves the analysis of single material benchmark experiments by the Monte Carlo code MCBEND (3) whilst the second stage will involve analysis of experiments consisting of simple representations of practical shield configurations with several materials. During 1992/1993 two such single material benchmarks have been analysed: an iron benchmark and a water benchmark. This report describes the analysis of the Winfrith water benchmark experiment. A separate report (4) describes the analysis of the iron benchmark.

In a water benchmark experiment attention can be more sharply focussed on the quality of the cross-section data than in benchmark experiments for most other materials. This is because the short migration length of fission energy neutrons in water means that an effectively infinite medium experiment and calculation can be carried out.

2. EXPERIMENT

2.1 The Experimental Arrangement

The general arrangement of the experiment is shown schematically in figure 1. A light structure supports a vertical aluminium tube in which the measurements are made. The eight arms of the support structure are used to suspend the Californium-252 neutron sources at predetermined and accurately known distances from the axis of the measurement tube; all sources are suspended at equal distances from the arms and measurements are made in the source plane and at distances 15cm and 30cm above and below the source plane in the air filled measurement tube. The support structure is located in a water-filled tank of cross-section 228cm x 177cm and height 172cm. The nearest distance of a source to any external boundary during any measurement was approximately 38cm; this is more than four times the migration length of 5MeV neutrons in water and therefore the whole source-detector arrangement can safely be treated as being immersed in an infinite bath of water.

Figure 2 shows in detail the source-detector arrangement with one source at the minimum separation distance of 10.16cm from the centre of the detector. This separation distance can be increased in units of 5.08cm and up to eight sources can be positioned symmetrically about the detector. The inner californium source capsule is contained by double stainless steel walls of total thickness 1.6mm and inserted via a

plug (not shown in the Figure) into an outer cylindrical stainless steel container. The neck of the outer container contains a steel screw which is connected by a very fine steel wire to an arm of the support structure. The central region of the source capsule contains a very small amount of air and aluminium. An exact geometric model of the source is given in Figure 3. The small amount of air and aluminium is treated as californium.

Absolute calibration of the sources was carried out at the National Physical Laboratory, Teddington, in April 1981. The source spectrum is shown in Table 1. The estimated standard deviation on the source strengths is 0.5% and in the results quoted in section 2.2 the appropriate (and very small) corrections for half life have been made. The angular variation of neutron output was measured by the National Physical Laboratory for one source and the results are shown in Figure 4.

Measurements were made of the S32(n,p)P32 reaction rate with sulphur detectors which were cast into cylindrical blocks of the same nominal size but whose dimensions vary slightly. The nominal size sample is shown in Figure 2. The cast sulphur samples had a density of 1.86±5% g/cm^3.

The neutron spectrum above 1MeV was also measured for each source-detector separation using a 3ml NE213 organic liquid scintillator located in the measurement tube, at source height.

2.2 The Measurements

The S32(n,p)P32 saturated reaction rates per sulphur atom per source neutron for the various source-detector separations are listed in Table 4. The 6% standard deviation shown for these measurements is caused by dispersion arising from the experimental method rather than from counting statistics. (The experimental values given for the off axis positions are the mean of the above and below axis measurements.)

The spectra unfolded using RADAK (5) from the pulse height spectra of a 3ml NE213 organic liquid scintillator at seven different source-detector separations are listed in Tables 6 to 12. These results are appropriate to the total source strengths given in Table 2. The standard deviation shown arises from random counting statistics, which varies from around 10% near 10MeV falling to 1-2% at about 4MeV and all lower energies, and a 5% contribution attributable to uncertainty in the volume of the detector. (This is systematic throughout the measurements.)

3. MCBEND MODEL

The experiment was analysed using version 7B of the Monte Carlo code MCBEND (3). The geometry described above and in Figures 1 to 3 was modelled using CG geometry. The measurements were made for seven different source-detector separations and varying numbers of sources (Table 2). Case 1 has one source capsule located 10.16cm from the detector; cases 2 and 3 have two and four sources respectively located symmetrically about the detector; and the remaining cases have all eight capsules. A source capsule was represented by a "cell" which could be replicated at the different locations for each case. The cell contained the bodies shown in Figure 3.

The material compositions used in the model are shown in Table 3. Uranium-238 was used to represent californium-252 which is not included in the MCBEND JEF2.2 library. Iron, nickel and chromium are present in the library in isotopic form only and so the composition of steel is defined using the relevant isotopes

Scoring regions were placed at source height and at distances of 15cm and 30cm above and below the source plane. Each scoring region was of height and diameter 2.8cm similar to the sulphur detector shown in Figure 2.

Acceleration of the code was provided by the method of splitting/Russian roulette, with importances derived using the CALCULATE option (6) which obtains the adjoint solution of the diffusion equation with adjusted diffusion coefficients. Splitting planes were placed every 5cm between source and detector. The acceleration was optimised for the S32(n,p)P32 reaction and targetted the detector at source height. The importance function for splitting was also used for source weighting.

In addition to the calculation of the fluxes and S32(n,p)P32 reaction rates the contributions from different energy groups to the response and the sensitivities of the detector response to changes in the material cross-sections were also scored.

The fluxes were scored in the energy group scheme in which the NE213 measurements were unfolded. Particles were not tracked below the sulphur threshold of 0.639MeV. The response function for sulphur was taken from the MCBEND response library which is sourced from IRDF 85 (7).

4. RESULTS

4.1 S32(n,p)P32 Reaction

Table 4 shows both the measured and calculated values of the sulphur reaction rate per source neutron at all locations. The measured values quoted at ±15cm and ±30cm from the source plane are obtained by averaging the above and below axis

measurements. In Table 5 the calculated off axis values have also been averaged in the same way. (Sulphur measurements were not made for source-detector spacings of 20.32 and 50.8cm.) The standard deviation on the calculated values, which is due to Monte Carlo stochastic error, increases away from the source plane because the calculation was targetted on this plane. The ratio of calculated to measured reaction rate (C/M) lies between 1.06 and 1.18 for the source plane and between 1.00 and 1.20 at ±15cm and ±30cm for the average results shown in Table 5. The majority of these calculated results lie within two standard deviations of the measurement so the MCBEND calculation with JEF2.2 cross-section data gives results which are generally consistent with experiment. There is however a tendency to overpredict the result.

Figure 5 shows the values of C/M in the source plane plotted against source-detector spacing. There is no clear evidence of a significant trend; at most it suggests the possibility of a small increase in C/M with source detector spacing.

Figure 6 illustrates the axial variation of reaction rate. The calculations predict the same axial profile as the measurement with the reaction rate becoming more uniform with increasing source-detector spacing, as expected. Figure 7 shows the values of reaction rate in the source plane multiplied by (source-detector spacing)^2 plotted against source-detector spacing. Both calculated and measured values lie on straight lines showing an exponential relationship. The calculated line is displaced slightly from the experimental line with a small decrease in gradient.

4.2. Neutron spectra above 1MeV

Tables 6 to 12 show the measured and calculated values of flux per unit lethargy for each source-detector separation and the corresponding values of C/M. (The lethargy width is the same for all groups in this scheme.) The percentage contribution to the sulphur reaction rate from each energy group is also tabulated. The standard deviation for the calculated values tends to be high for results below 1.7MeV. This is because the calculation was targetted on the S32(n,p)P32 reaction which has a cross-section which decreases very sharply below 2MeV. The calculated standard deviations are quite high around 10MeV where the contribution to the sulphur reaction rate is small, again because the calculation was targetted on this reaction.

Figures 8 to 14 show the neutron spectra and Figures 15 to 21 show the values of C/M plotted against energy. (Values with a standard deviation greater than 20% have been omitted.) In general there is good agreement over the energy range 1.5 to 8.8MeV with C/M in the range 0.8 to 1.3 and the majority of calculated values lie within two standard deviations of the measurement. Above 8.8MeV the MCBEND calculation with JEF2.2 data severely overpredicts the flux at source-detector spacings up to 35.56cm;

at 50.8cm the calculation is consistent with measurement. Below 1.5MeV the MCBEND calculation underpredicts the flux by at least a factor of 2; however it is possible that the results at these lower energies are misleading because neutrons of these energies have been poorly sampled as they would provide only a small contribution to the sulphur reaction rate.

The percentage contributions to sulphur response indicate that, as the source-detector spacing increases, the bulk of the contributions move to higher energies i.e at 10.16cm 67% of the response comes from 2.86 to 6.06MeV whereas for a spacing of 50.8cm 68% comes from 3.67 to 7.78MeV.

5. DISCUSSION

Below 13MeV the total macroscopic cross-section for hydrogen in water is greater than that of oxygen even at the narrow resonance peaks in oxygen. At 8MeV the cross-section is twice as large for hydrogen as for oxygen and at lower energies the average ratio is even higher. Therefore most of the collisions in water are with hydrogen nuclei. Further, an elastic collision with oxygen does not significantly degrade the neutron and does not appreciably change the neutron direction. The cross-section is mainly due to small angle elastic scattering which has little effect on the penetration; and it does not show an appreciable absorption component. Collisions with hydrogen, on the other hand, will tend to degrade the neutron energy so much as to remove it from the MeV region. Hydrogen collisions therefore play the dominant role in the penetration of fast neutrons through water. Hence calculations performed for the water benchmark can be used to validate hydrogen cross-section data.

Table 14 shows the sensitivity of the S32(n,p)P32 response to changes in total cross-section of H, O and Fe56 for cases 1 and 7, the smallest and largest source-detector spacings. For all other nuclides the sensitivities were found to be negligible. These results confirm that hydrogen plays the dominant role in these experiments.

The hydrogen cross-section decreases with increasing energy and therefore for greater source-detector spacings, higher energy neutrons are more important. This is confirmed by the results from the contributions to sulphur response.

6. COMPARISON WITH MCBEND RESULTS USING UKNDL DATA

A MCBEND calculation has been performed for the water benchmark using UKNDL cross-section data for a source-detector spacing of 35.56cm only (case 6). The result for the S32(n,p)P32 reaction rate is shown in figure 7 along with the

experiment and JEF2.2 results. The UKNDL calculation also overpredicts the reaction rate and the agreement is similar to calculations with JEF2.2 data.

Table 13 shows the calculated neutron spectrum and values of C/M for each energy group. This can be compared with Table 11, the corresponding results for JEF2.2 data. The two sets of results are also shown in figure 13. There is no major difference between the spectra calculated with the two sets of cross-section data.

7. DISCUSSION OF ERRORS

(i) The Source Definition

The NPL calibration of the sources was for each source within its capsule and therefore the values of source strength quoted in Table 2 refer to the emission of neutrons from the capsule not from the californium as used in the model. However it was necessary to model the capsule to predict the anisotropy of the source and modification of the spectrum produced by attenuation through steel. A further MCBEND calculation was performed to assess the error this introduced. The model consisted of a single source capsule in a void with a 1cm thick spherical scoring region 1m from the centre of the source. Neutrons, at this distance, will be generally moving in a radial direction and it is possible to compare the calculated flux with that due to a point source. This would provide a correction factor to compensate for absorption of neutrons within the capsule.

$$\text{Flux due to a point source} = \frac{1.256E7}{4\pi(100.5^2)} = 98.957 \text{ n cm}^{-2} \text{ s}^{-1}$$

Total calculated flux (12.84 to 1.0E-20MeV) = 97.94 n cm^{-2} s^{-1} (st.dev. 0.1%)

$$\frac{98.957}{97.94} = 1.0104 \quad \text{(st.dev. 0.1\%)}$$

Therefore the results for both sulphur reaction rate and spectra quoted in tables 4 to 13 should be 1% higher.

The source spectrum is well defined (8, 9, 10) and refers to the spectrum from the californium inside the capsule.

(ii) The Sulphur detectors

In the MCBEND model the scoring regions were represented by void to allow calculation of both spectra and sulphur reaction rate for comparison with experiment. However the sulphur detectors were relatively large (height and diameter 2.8cm) and would attenuate the neutrons further such that the calculated results would be too high.

A further MCBEND calculation was performed, for case 5, with the scoring regions represented by sulphur of density 1.86g/cm^3 and the sensitivity of the response to the total sulphur cross-section was calculated. This indicated that removal of sulphur would give an increase in reaction rate of ~3%. Therefore the results quoted in Tables 4 and 5 for the S32(n,p)P32 reaction rate are ~3% too high.

(iii) JEF2.2 Cross-Sections

Errors for JEF2.2 cross-section data were not readily available but values for JEF1 data, in the Weisbin group scheme, were available and these can be considered typical. The errors for hydrogen and oxygen were folded in with the sensitivity data (Table 14) to calculate the overall error in sulphur response due to the cross-section data. This was 0.5% and 5.0% for source-detector spacings of 10.16 and 50.8cm respectively.

The error in the calculated S32(n,p)P32 reaction rate due to errors in cross-section data increases from 0.5% to 5% over the range of source-detector spacings analysed. However there was no clear trend in the results with penetration which could be explained by this increasing error.

(iv) Location of the sources

The error in the source-detector separation quoted in Figure 2 is ±0.25mm. The change in sulphur reaction rate for this small change in distance is negligible (see Figure 7). The error in height of the source is ±0.4mm. Figure 6 shows that the change in reaction rate over this axial range is not significant.

In summary the MCBEND model introduces systematic errors of -1% and +3% in the sulphur reaction rate from treatment of the source and detector respectively giving results which are ~2% too high. The accuracy of the cross-section data introduces an error of ±0.5% to ±5.0% over the range of source-detector spacings considered.

8. CONCLUSIONS

The water benchmark experiment provides a geometry which can be modelled accurately and so geometry approximations do not introduce inaccuracy into the results.

In general MCBEND calculations with JEF2.2 cross-section data slightly overpredict the S32(n,p)P32 reaction rate with C/M in the range 1.0 to 1.20. The majority of results lie within two standard deviations of the measurements and so are individually consistent with measurement but the small trend towards overprediction

appears to be significant. There is, however, no clear evidence that it increases with penetration distance. The calculated spectra are in good agreement over the range 1.7 to 8.8MeV with C/M lying mainly between 0.8 and 1.3 and within 2 standard deviations of unity. Around 10MeV the calculated flux is too high. Below 1.7MeV the calculated flux is lower than measurement by a factor of ~2; however these results may be misleading because neutrons of these energies have been poorly sampled. Further calculations are necessary targetting these energies for verification.

Thus JEF2.2 cross-section data for hydrogen and oxygen are valid for use in Monte Carlo calculations using MCBEND for neutron energies in the range 1.7 to 8.8MeV.

REFERENCES

1. C. Nordborg, H. Gruppelaar and M. Salvatores
Status of the JEF and EFF Projects.
Proc. International Conference on Nuclear Data for Science and Technology, Fed. Rep. Germany May 1991

2. C. Nordborg
Distribution of JEF2.2
JEF/DOC371

3. MCBEND User guide
ANSWERS/MCBEND(91)7

4. G.A. Wright and M.J. Grimstone
Benchmark Testing of JEF2.2 Data for Shielding Applications: Analysis of the Winfrith Iron-88 Benchmark Experiment.
AEA-RS-1231 (1993)

5. Grimstone M.J.
The RADAK User's Manual
AEEW-M-1455 (1976)

6. P.C.Miller, C.B.Boyle, S.W.Power and G.A.Wright
The Use of an inbuilt importance generator for acceleration of the Monte Carlo code MCBEND.
International conference on the Physics of Reactors: Operation, Design and Computation, Marseille, France. April 1990.

7. D.E.Cullen and P.K.McLaughlin
"The International Reactor Dosimetry File (IRDF85)"
IAEA-ND5-41

8. P.I.Johansson et al
Bull. Am. Phys. Soc. 20, 159, GB8 (1975)

9. H.H.Knitter et al
IAEA Vienna Consultants' Meeting on Prompt Fission Spectra (1971) NEANDC (E) - 161 U 208

10. Grundl J and Eisenhauer C
ERDA-NDC-3U, 159 (May 1976)

Table 1. Californium-252 Neutron Source Spectrum

Upper Energy (MeV)	Neutrons per second	Upper Energy (MeV)	Neutrons per second
1.284E+01	7.119E-04	8.208E-01	2.945E-02
1.133E+01	1.625E-03	7.244E-01	3.097E-02
1.000E+01	3.304E-03	6.393E-01	2.747E-02
8.825E+00	6.059E-03	5.642E-01	2.417E-02
7.788E+00	1.014E-02	4.979E-01	2.112E-02
6.873E+00	1.565E-02	4.394E-01	1.833E-02
6.065E+00	2.222E-02	3.877E-01	1.583E-02
5.353E+00	2.941E-02	3.422E-01	1.361E-02
4.724E+00	3.684E-02	3.020E-01	1.164E-02
4.169E+00	4.398E-02	2.655E-01	9.835E-03
3.679E+00	5.033E-02	2.352E-01	8.134E-03
3.247E+00	5.547E-02	2.075E-01	6.660E-03
2.865E+00	5.914E-02	1.832E-01	5.456E-03
2.528E+00	6.123E-02	1.616E-01	4.473E-03
2.231E+00	6.177E-02	1.426E-01	3.670E-03
1.969E+00	6.090E-02	1.259E-01	3.014E-03
1.738E+00	5.884E-02	1.111E-01	2.476E-03
1.534E+00	4.715E-02	9.804E-02	2.036E-03
1.353E+00	3.633E-02	8.652E-02	1.676E-03
1.194E+00	3.329E-02	7.635E-02	1.380E-03
1.054E+00	3.015E-02	6.738E-02	1.137E-03
9.301E-01	2.702E-02	5.946E-02	
			1.0

Table 2. Experimental Source Arrangements.

CASE	source-detector spacing (cm)	Number of sources	Total source strength (n/s)
1	10.16	1	1.2560E+07
2	15.24	2	2.5400E+07
3	20.32	4	5.2600E+07
4	25.40	8	1.0480E+08
5	30.48	8	1.0460E+08
6	35.56	8	1.0484E+08
7	50.80	8	1.0445E+08

Table 3. Material Compositions.

Composition	Proportion by weight	Density (g/cm^3)	JEF2.2 MOULD/DFN	UKNDL MOULD/DFN
U238	1.0	18.7	9237 / 114	2 / 160
Al	1.0	2.7	2 / 1325	8 / 935
Mn	1.587E-02	7.9	41 / 2525	34 / 88
Fe54	4.010E-02		26 / 2625	10 / 908
Fe56	6.458E-01		27 / 2631	10 / 908
Fe57	1.500E-02		28 / 2634	10 / 908
Fe58	2.100E-03		29 / 2637	10 / 908
Cr50	7.800E-03		19 / 2425	13 / 446
Cr52	1.564E-01		20 / 2431	13 / 446
Cr53	1.800E-02		21 / 2434	13 / 446
Cr54	4.600E-03		22 / 2437	13 / 446
Ni58	6.387E-02		51 / 2825	14 / 907
Ni60	2.545E-02		52 / 2831	14 / 907
Ni61	1.120E-03		53 / 2834	14 / 907
Ni62	3.640E-03		54 / 2837	14 / 907
Ni64	9.600E-04		55 / 2843	14 / 907
H	1.119E-01	1.0	97 / 10293	7 / 923
O	8.881E-01		56 / 825	43 / 933

Table 4. S32(n,p)P32 Reaction rates at all locations

Axial Displacement	Calculated Response			Experiment	
	(Bq/barn)	(Bq/atom/source neutron)	sd (%)	(Bq/atom/source neutron)	sd (%)
1. Source = 1.256E7 n/s 10.16cm from detector					
30.0	9.690E+00	7.71E-31	19.7	6.71E-31	6.0
15.0	6.849E+01	5.45E-30	6.0	5.37E-30	6.0
0.0	4.181E+02	3.33E-29	2.2	3.13E-29	6.0
-15.0	6.652E+01	5.30E-30	6.2	5.37E-30	6.0
-30.0	7.177E+00	5.71E-31	14.1	6.71E-31	6.0
2. Source = 2.540E7 n/s 15.24cm from detector					
30.0	9.726E+00	3.83E-31	9.3	3.22E-31	6.0
15.0	6.731E+01	2.65E-30	4.8	2.25E-30	6.0
0.0	2.193E+02	8.63E-30	2.2	7.56E-30	6.0
-15.0	6.143E+01	2.42E-30	3.6	2.25E-30	6.0
-30.0	8.184E+00	3.22E-31	6.9	3.22E-31	6.0
3. Source = 5.260E7 n/s 20.32cm from detector					
30.0	1.002E+01	1.90E-31	6.5		
15.0	6.022E+00	1.14E-31	3.3		
0.0	1.349E+02	2.56E-30	2.6		
-15.0	5.839E+01	1.11E-30	3.2		
-30.0	9.617E+00	1.83E-31	6.7		
4. Source = 1.048E7 n/s 25.40cm from detector					
30.0	1.012E+01	9.66E-32	6.2	9.50E-32	6.0
15.0	5.289E+01	5.05E-31	3.1	4.36E-31	6.0
0.0	1.055E+02	1.01E-30	2.8	8.55E-31	6.0
-15.0	5.263E+01	5.02E-31	3.0	4.36E-31	6.0
-30.0	1.083E+01	1.03E-31	5.9	9.50E-32	6.0
5. Source = 1.046E7 n/s 30.48cm from detector					
30.0	6.410E+00	6.13E-32	9.2	5.16E-32	6.0
15.0	2.434E+01	2.33E-31	4.3	1.94E-31	6.0
0.0	4.050E+01	3.87E-31	3.6	3.43E-31	6.0
-15.0	2.416E+01	2.31E-31	3.8	1.94E-31	6.0
-30.0	6.526E+00	6.24E-32	9.2	5.16E-32	6.0
6. Source = 1.048E7 n/s 35.56cm from detector					
30.0	3.426E+00	3.27E-32	9.8	2.81E-32	6.0
15.0	1.030E+01	9.82E-32	4.3	8.92E-32	6.0
0.0	1.693E+01	1.61E-31	3.8	1.42E-31	6.0
-15.0	1.048E+01	1.00E-31	4.3	8.92E-32	6.0
-30.0	3.652E+00	3.48E-32	9.9	2.81E-32	6.0
7. Source = 1.045E7 n/s 50.80cm from detector					
30.0	5.516E-01	5.28E-33	8.0		
15.0	1.169E+00	1.12E-32	3.2		
0.0	1.544E+00	1.48E-32	2.9		
-15.0	1.174E+00	1.12E-32	3.3		
-30.0	4.936E-01	4.73E-33	7.8		

Table 5. Average Axial Results for S32(n,p)P32 Reaction rates.

Axial Displacement	Experiment		Calculated Response		C/M	error
	(Bq/atom/source neutron)	sd (%)	(Bq/atom/source neutron)	sd (%)		sd
1. Source = 1.256E7 n/s 10.16cm from detector						
±30.0	6.71E-31	6.0	6.71E-31	12.81	1.00	0.14
±15.0	5.37E-30	6.0	5.37E-30	4.31	1.00	0.07
0.0	3.13E-29	6.0	3.33E-29	2.20	1.06	0.07
2. Source = 2.540E7 n/s 15.24cm from detector						
±30.0	3.22E-31	6.0	3.53E-31	5.95	1.09	0.09
±15.0	2.25E-30	6.0	2.53E-30	3.04	1.13	0.08
0.0	7.56E-30	6.0	8.63E-30	2.20	1.14	0.07
3. Source = 5.260E7 n/s 20.32cm from detector						
±30.0			1.87E-31	4.67		
±15.0			6.12E-31	2.92		
0.0			2.56E-30	2.60		
4. Source = 1.048E7 n/s 25.40cm from detector						
±30.0	9.50E-32	6.0	1.00E-31	4.27	1.05	0.08
±15.0	4.36E-31	6.0	5.03E-31	2.16	1.15	0.07
0.0	8.55E-31	6.0	1.01E-30	2.80	1.18	0.08
5. Source = 1.046E7 n/s 30.48cm from detector						
±30.0	5.16E-32	6.0	6.18E-32	6.51	1.20	0.11
±15.0	1.94E-31	6.0	2.32E-31	2.87	1.20	0.08
0.0	3.43E-31	6.0	3.87E-31	3.60	1.13	0.08
6. Source = 1.048E7 n/s 35.56cm from detector						
±30.0	2.81E-32	6.0	3.38E-32	6.97	1.20	0.11
±15.0	8.92E-32	6.0	9.91E-32	3.04	1.11	0.07
0.0	1.42E-31	6.0	1.61E-31	3.80	1.14	0.08
7. Source = 1.045E7 n/s 50.80cm from detector						
±30.0			5.00E-33	5.60		
±15.0			1.12E-32	2.30		
0.0			1.48E-32	2.90		

Table 6. Neutron Spectrum at 10.16cm.

		Flux per unit lethargy (n/cm²/s)						% contribution to S32 response
Group	Emax (MeV)	Calculation	sd (%)	Experiment	sd (%)	C/M	error	
1	10	2.28E+02	9.1	8.50E+01	14.5	2.68	0.46	2.72
2	8.825	2.77E+02	9.0	2.07E+02	10.3	1.34	0.18	2.94
3	7.788	4.41E+02	7.3	3.45E+02	8.0	1.28	0.14	4.53
4	6.873	7.56E+02	6.0	5.80E+02	6.7	1.30	0.12	7.67
5	6.065	9.22E+02	5.9	8.36E+02	5.8	1.10	0.09	8.70
6	5.353	1.19E+03	5.5	1.15E+03	5.6	1.03	0.08	9.32
7	4.724	1.42E+03	6.0	1.33E+03	5.4	1.07	0.09	13.46
8	4.169	1.77E+03	5.8	1.70E+03	5.2	1.04	0.08	13.53
9	3.679	1.83E+03	7.7	1.82E+03	5.3	1.01	0.09	11.81
10	3.247	2.42E+03	8.5	2.25E+03	5.2	1.08	0.11	10.35
11	2.865	2.13E+03	10.3	2.61E+03	5.2	0.81	0.09	5.70
12	2.528	2.83E+03	11.8	2.68E+03	5.1	1.06	0.14	6.83
13	2.231	2.09E+03	10.9	2.64E+03	5.4	0.79	0.10	1.91
14	1.969	2.25E+03	13.0	2.48E+03	5.3	0.91	0.13	0.47
15	1.738	1.21E+03	64.4	2.49E+03	5.4	0.49	0.31	0.05
16	1.534	7.24E+02	46.3	2.54E+03	5.4	0.28	0.13	0.01
17	1.353	6.42E+02	51.5	2.26E+03	6.0	0.28	0.15	0.00
18	1.194	2.46E+02	7.0	2.34E+03	6.0	0.11	0.01	0.00
19	1.054	9.40E+02	74.7	2.02E+03	5.5	0.47	0.35	0.00

Table 7. Neutron Spectrum at 15.24cm.

		Flux per unit lethargy (n/cm²/s)						% contribution to S32 response
Group	Emax (MeV)	Calculation	sd (%)	Experiment	sd (%)	C/M	error	
1	10	1.32E+02	9.6	6.78E+01	10.5	1.94	0.28	2.97
2	8.825	1.38E+02	10.1	1.12E+02	8.7	1.24	0.16	2.80
3	7.788	2.21E+02	8.2	2.12E+02	6.2	1.04	0.11	4.32
4	6.873	3.59E+02	7.0	3.59E+02	5.8	1.00	0.09	6.94
5	6.065	5.01E+02	6.0	4.57E+02	5.8	1.10	0.09	9.03
6	5.353	7.49E+02	5.2	5.98E+02	5.4	1.25	0.09	11.20
7	4.724	7.29E+02	6.1	7.77E+02	5.2	0.94	0.08	13.18
8	4.169	9.09E+02	5.6	7.84E+02	5.3	1.16	0.09	12.85
9	3.679	8.76E+02	6.3	8.64E+02	5.3	1.01	0.08	10.59
10	3.247	1.13E+03	7.5	1.10E+03	5.1	1.03	0.09	9.27
11	2.865	1.67E+03	12.3	1.23E+03	5.1	1.35	0.18	8.02
12	2.528	1.36E+03	11.8	1.38E+03	5.2	0.99	0.13	6.29
13	2.231	1.22E+03	10.9	1.21E+03	5.3	1.01	0.12	2.13
14	1.969	9.51E+02	9.1	1.13E+03	5.2	0.84	0.09	0.35
15	1.738	5.68E+02	7.5	1.18E+03	5.1	0.48	0.04	0.05
16	1.534	5.44E+02	7.5	1.15E+03	5.1	0.47	0.04	0.01
17	1.353	5.82E+02	10.8	9.83E+02	5.3	0.59	0.07	0.00
18	1.194	4.95E+02	8.6	1.09E+03	5.2	0.45	0.05	0.00
19	1.054	4.09E+02	7.7	8.86E+02	5.1	0.46	0.04	0.00

Table 8. Neutron Spectrum at 20.32cm.

		Flux per unit lethargy (n/cm²/s)						% contribution to S32 response
Group	Emax (MeV)	Calculation	sd (%)	Experiment	sd (%)	C/M	error	
1	10	1.12E+02	11.9	5.49E+01	8.6	2.05	0.30	4.23
2	8.825	1.02E+02	13.9	8.53E+01	7.8	1.19	0.19	3.34
3	7.788	1.45E+02	10.4	1.56E+02	6.3	0.93	0.11	6.29
4	6.873	2.70E+02	9.0	2.49E+02	5.7	1.08	0.12	6.65
5	6.065	3.44E+02	7.7	3.19E+02	5.8	1.08	0.10	10.84
6	5.353	4.50E+02	7.1	4.39E+02	5.4	1.02	0.09	9.61
7	4.724	4.87E+02	8.5	4.81E+02	5.3	1.01	0.10	15.33
8	4.169	4.75E+02	6.4	5.05E+02	5.3	0.94	0.08	12.57
9	3.679	4.93E+02	5.9	5.11E+02	5.3	0.97	0.08	8.38
10	3.247	7.12E+02	7.8	6.80E+02	5.2	1.05	0.10	9.52
11	2.865	6.27E+02	9.8	7.54E+02	5.1	0.83	0.09	5.28
12	2.528	8.39E+02	12.5	8.56E+02	5.0	0.98	0.13	5.81
13	2.231	6.75E+02	9.9	7.45E+02	5.1	0.91	0.10	1.73
14	1.969	7.43E+02	11.1	7.08E+02	5.2	1.05	0.13	0.36
15	1.738	5.22E+02	11.3	6.70E+02	5.2	0.78	0.10	0.03
16	1.534	5.70E+02	11.4	7.03E+02	5.1	0.81	0.10	0.02
17	1.353	4.97E+02	32.1	6.03E+02	5.2	0.82	0.27	0.00
18	1.194	3.51E+02	10.9	6.85E+02	5.2	0.51	0.06	0.00
19	1.054	2.79E+02	11.6	5.65E+02	5.2	0.49	0.06	0.00

Table 9. Neutron Spectrum at 25.40cm.

		Flux per unit lethargy (n/cm²/s)						% contribution to S32 response
Group	Emax (MeV)	Calculation	sd (%)	Experiment	sd (%)	C/M	error	
1	10	9.04E+01	13.4	3.92E+01	10.3	2.31	0.39	4.26
2	8.825	8.50E+01	13.7	7.50E+01	7.8	1.13	0.18	3.58
3	7.788	1.52E+02	10.9	1.20E+02	6.5	1.26	0.16	6.16
4	6.873	2.13E+02	9.8	1.92E+02	5.9	1.11	0.13	8.57
5	6.065	2.54E+02	7.8	2.55E+02	6.0	1.00	0.10	9.53
6	5.353	3.21E+02	6.8	3.18E+02	5.7	1.01	0.09	9.97
7	4.724	3.73E+02	7.9	3.54E+02	5.4	1.05	0.10	14.13
8	4.169	3.41E+02	5.8	3.62E+02	5.3	0.94	0.07	10.10
9	3.679	3.60E+02	5.7	3.43E+02	5.4	1.05	0.08	9.15
10	3.247	6.17E+02	9.9	4.44E+02	5.3	1.39	0.16	10.43
11	2.865	5.24E+02	9.1	5.30E+02	5.2	0.99	0.10	5.38
12	2.528	6.60E+02	17.4	5.80E+02	5.2	1.14	0.21	6.34
13	2.231	4.99E+02	10.6	5.20E+02	5.2	0.96	0.11	1.98
14	1.969	4.19E+02	5.2	4.73E+02	5.2	0.89	0.07	0.33
15	1.738	3.62E+02	15.0	4.75E+02	5.2	0.76	0.12	0.07
16	1.534	3.44E+02	13.9	4.77E+02	5.2	0.72	0.11	0.01
17	1.353	3.48E+02	14.5	4.40E+02	5.7	0.79	0.12	0.00
18	1.194	3.23E+02	13.9	5.21E+02	5.5	0.62	0.09	0.00
19	1.054	2.28E+02	13.2	4.26E+02	6.4	0.54	0.08	0.00

Table 10. Neutron Spectrum at 30.48cm.

		Flux per unit lethargy (n/cm²/s)						% contribution to S32 response
Group	Emax (MeV)	Calculation	sd (%)	Experiment	sd (%)	C/M	error	
1	10	3.22E+01	18.5	1.85E+01	8.9	1.74	0.36	3.98
2	8.825	3.22E+01	20.9	3.19E+01	6.7	1.01	0.22	3.53
3	7.788	6.10E+01	14.8	5.71E+01	5.6	1.07	0.17	6.46
4	6.873	9.01E+01	13.0	8.41E+01	5.6	1.07	0.15	9.44
5	6.065	1.11E+02	10.6	1.02E+02	5.5	1.09	0.13	10.81
6	5.353	1.53E+02	9.8	1.29E+02	5.2	1.19	0.13	12.40
7	4.724	1.61E+02	10.2	1.42E+02	5.2	1.13	0.13	15.74
8	4.169	1.22E+02	6.5	1.32E+02	5.2	0.92	0.08	9.49
9	3.679	1.12E+02	4.5	1.26E+02	5.2	0.89	0.06	7.58
10	3.247	1.65E+02	9.4	1.65E+02	5.1	1.00	0.11	7.48
11	2.865	1.59E+02	8.8	1.89E+02	5.1	0.84	0.09	4.32
12	2.528	2.77E+02	15.9	2.13E+02	5.1	1.30	0.22	6.85
13	2.231	1.65E+02	7.5	1.83E+02	5.2	0.90	0.08	1.68
14	1.969	1.80E+02	10.1	1.69E+02	5.2	1.07	0.12	0.39
15	1.738	1.37E+02	23.5	1.64E+02	5.2	0.84	0.20	0.06
16	1.534	1.55E+02	23.4	1.66E+02	5.1	0.93	0.22	0.02
17	1.353	1.77E+02	24.3	1.52E+02	5.3	1.16	0.29	0.01
18	1.194	1.18E+02	23.2	1.82E+02	5.2	0.65	0.15	0.00
19	1.054	1.69E+02	49.7	1.69E+02	5.0	1.00	0.50	0.00

Table 11. Neutron Spectrum at 35.56cm.

		Flux per unit lethargy (n/cm²/s)						% contribution to S32 response
Group	Emax (MeV)	Calculation	sd (%)	Experiment	sd (%)	C/M	error	
1	10	1.76E+01	19.8	9.62E+00	10.3	1.83	0.41	5.12
2	8.825	1.63E+01	22.5	1.45E+01	8.9	1.12	0.27	4.29
3	7.788	2.60E+01	16.2	2.47E+01	6.9	1.05	0.19	6.59
4	6.873	3.53E+01	14.4	3.59E+01	6.7	0.98	0.16	8.86
5	6.065	4.40E+01	12.8	4.25E+01	6.3	1.04	0.15	10.30
6	5.353	6.77E+01	12.1	5.60E+01	5.6	1.21	0.16	13.14
7	4.724	5.73E+01	6.7	5.67E+01	5.5	1.01	0.09	13.42
8	4.169	6.25E+01	7.4	5.38E+01	5.5	1.16	0.11	11.83
9	3.679	4.98E+01	5.8	4.46E+01	6.3	1.12	0.10	7.82
10	3.247	6.90E+01	13.2	6.38E+01	5.7	1.08	0.16	7.41
11	2.865	6.95E+01	14.3	6.92E+01	5.6	1.00	0.15	4.67
12	2.528	8.18E+01	11.6	7.95E+01	5.5	1.03	0.13	4.80
13	2.231	5.41E+01	7.9	6.74E+01	5.4	0.80	0.08	1.29
14	1.969	6.07E+01	10.2	6.25E+01	5.4	0.97	0.11	0.31
15	1.738	8.07E+01	75.5	6.00E+01	5.5	1.35	1.02	0.13
16	1.534	4.00E+01	61.7	5.99E+01	5.4	0.67	0.41	0.01
17	1.353	2.61E+01	35.5	5.43E+01	5.2	0.48	0.17	0.00
18	1.194	2.06E+01	36.9	6.49E+01	5.0	0.32	0.12	0.00
19	1.054	3.05E+01	41.3	5.64E+01	5.0	0.54	0.22	0.00

Table 12. Neutron Spectrum at 50.80cm.

		Flux per unit lethargy (n/cm²/s)						% contribution to S32 response
Group	Emax (MeV)	Calculation	sd (%)	Experiment	sd (%)	C/M	error	
1	10	1.71E+00	15.2	1.43E+00	9.7	1.20	0.22	5.48
2	8.825	1.88E+00	16.4	1.85E+00	11.4	1.01	0.20	5.41
3	7.788	2.81E+00	13.5	2.79E+00	10.1	1.01	0.17	7.82
4	6.873	4.71E+00	12.1	4.07E+00	8.1	1.16	0.17	12.93
5	6.065	4.69E+00	7.6	4.82E+00	7.9	0.97	0.11	11.96
6	5.353	5.61E+00	7.7	4.71E+00	8.1	1.19	0.13	11.94
7	4.724	5.19E+00	4.6	5.49E+00	6.9	0.94	0.08	13.38
8	4.169	4.72E+00	3.0	3.83E+00	7.4	1.23	0.10	9.78
9	3.679	3.76E+00	2.8	4.21E+00	6.3	0.89	0.06	6.47
10	3.247	5.04E+00	5.7	4.59E+00	5.9	1.10	0.09	5.88
11	2.865	5.65E+00	7.9	5.08E+00	6.1	1.11	0.11	4.11
12	2.528	5.27E+00	5.3	5.85E+00	6.4	0.90	0.07	3.43
13	2.231	4.31E+00	5.0	4.58E+00	7.6	0.94	0.09	1.13
14	1.969	3.98E+00	4.9	4.34E+00	7.7	0.92	0.08	0.21
15	1.738	2.61E+00	45.1	4.32E+00	6.5	0.60	0.28	0.04
16	1.534	1.57E+00	39.8	4.17E+00	5.6	0.38	0.15	0.00
17	1.353	4.25E+00	44.3	3.94E+00	5.3	1.08	0.48	0.00
18	1.194	2.40E+00	47.8	4.42E+00	5.1	0.54	0.26	0.00
19	1.054	2.00E+00	35.8	4.61E+00	6.0	0.43	0.16	0.00

Table 13. Neutron Spectrum at 35.56cm. (UKNDL data)

		Flux per unit lethargy (n/cm²/s)						% contribution to S32 response
Group	Emax (MeV)	Calculation	sd (%)	Experiment	sd (%)	C/M	error	
1	10	1.68E+01	17.1	9.62E+00	10.3	1.74	0.35	5.23
2	8.825	1.70E+01	16.9	1.45E+01	8.9	1.17	0.22	4.68
3	7.788	2.25E+01	11.6	2.47E+01	6.9	0.91	0.12	6.01
4	6.873	3.68E+01	10.8	3.59E+01	6.7	1.03	0.13	9.72
5	6.065	4.98E+01	9.3	4.25E+01	6.3	1.17	0.13	12.25
6	5.353	5.82E+01	7.6	5.60E+01	5.6	1.04	0.10	11.92
7	4.724	5.12E+01	5.1	5.67E+01	5.5	0.90	0.07	12.67
8	4.169	4.84E+01	5.5	5.38E+01	5.5	0.90	0.07	9.55
9	3.679	4.95E+01	4.2	4.46E+01	6.3	1.11	0.08	8.30
10	3.247	5.54E+01	2.9	6.38E+01	5.7	0.87	0.06	6.17
11	2.865	7.47E+01	8.9	6.92E+01	5.6	1.08	0.11	5.09
12	2.528	1.03E+02	18.7	7.95E+01	5.5	1.30	0.25	6.48
13	2.231	6.35E+01	8.8	6.74E+01	5.4	0.94	0.10	1.57
14	1.969	5.54E+01	4.5	6.25E+01	5.4	0.89	0.06	0.29
15	1.738	4.15E+01	24.9	6.00E+01	5.5	0.69	0.18	0.05
16	1.534	3.91E+01	22.4	5.99E+01	5.4	0.65	0.15	0.01
17	1.353	7.31E+01	33.4	5.43E+01	5.2	1.35	0.46	0.01
18	1.194	2.23E+01	24.4	6.49E+01	5.0	0.34	0.09	0.00
19	1.054	3.64E+01	31.0	5.64E+01	5.0	0.64	0.20	0.00

Table 14. Sensitivity of S32(n,p)P32 Response to changes in the Total cross-section of Hydrogen, Oxygen and Iron-56.

		H		O		Fe56	
Group	Upper Energy (MeV)	sensitivity	sd	sensitivity	sd	sensitivity	sd
Source - Detector Spacing = 10.16cm							
1	14.92	-0.188	0.010	0.004	0.009	-0.037	0.006
2	4.40	-0.317	0.015	-0.033	0.009	-0.022	0.007
3	2.60	-0.072	0.007	-0.009	0.001	-0.003	0.001
	1.35						
Source - Detector Spacing = 50.80cm							
Group	Upper Energy (MeV)	sensitivity	sd	sensitivity	sd	sensitivity	sd
1	14.92	-2.833	0.111	-0.917	0.051	-0.062	0.010
2	4.40	-0.836	0.039	-0.228	0.012	-0.005	0.001
3	2.60	-0.098	0.007	-0.010	0.001		
	1.35						

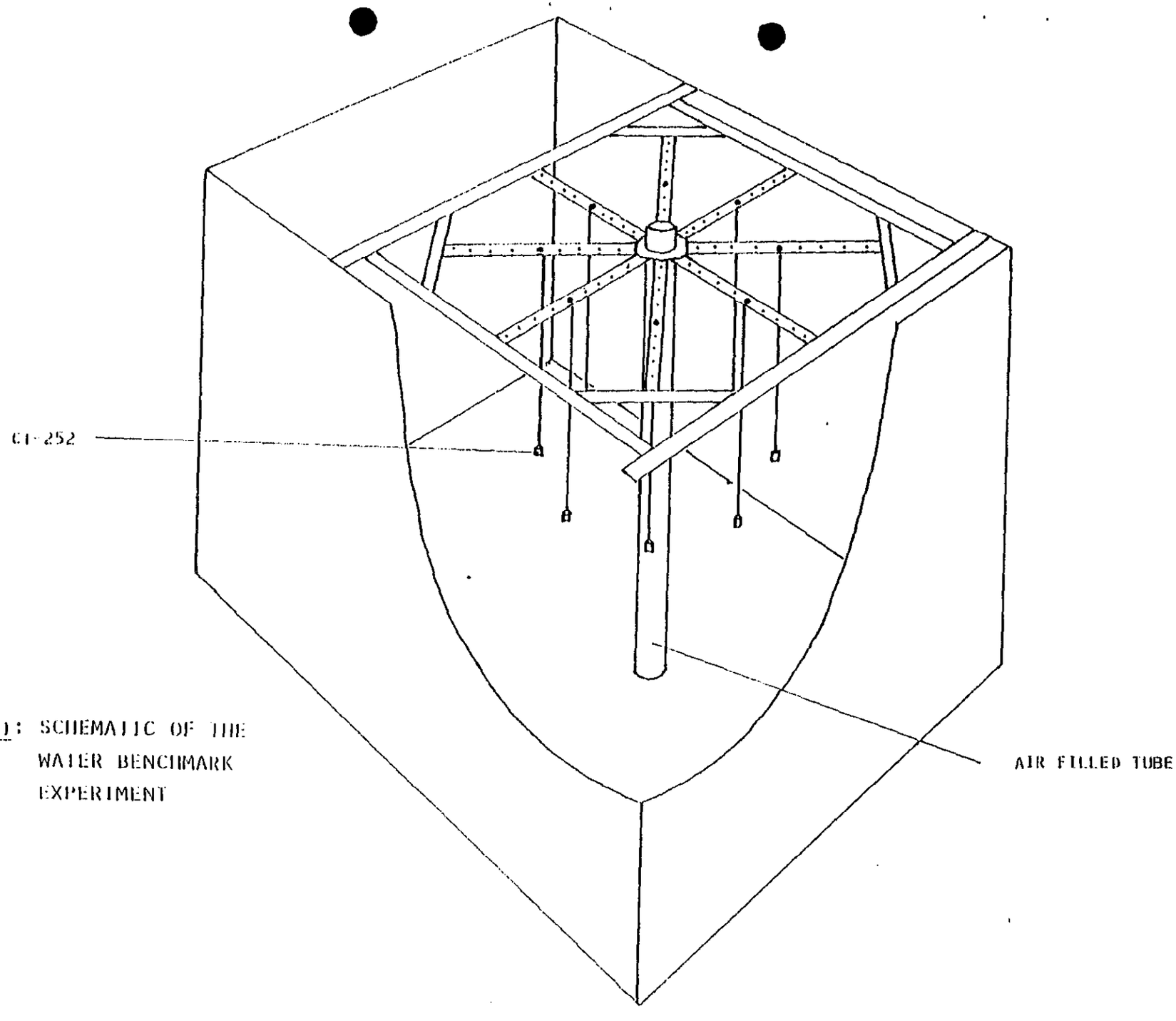

FIGURE 1: SCHEMATIC OF THE WATER BENCHMARK EXPERIMENT

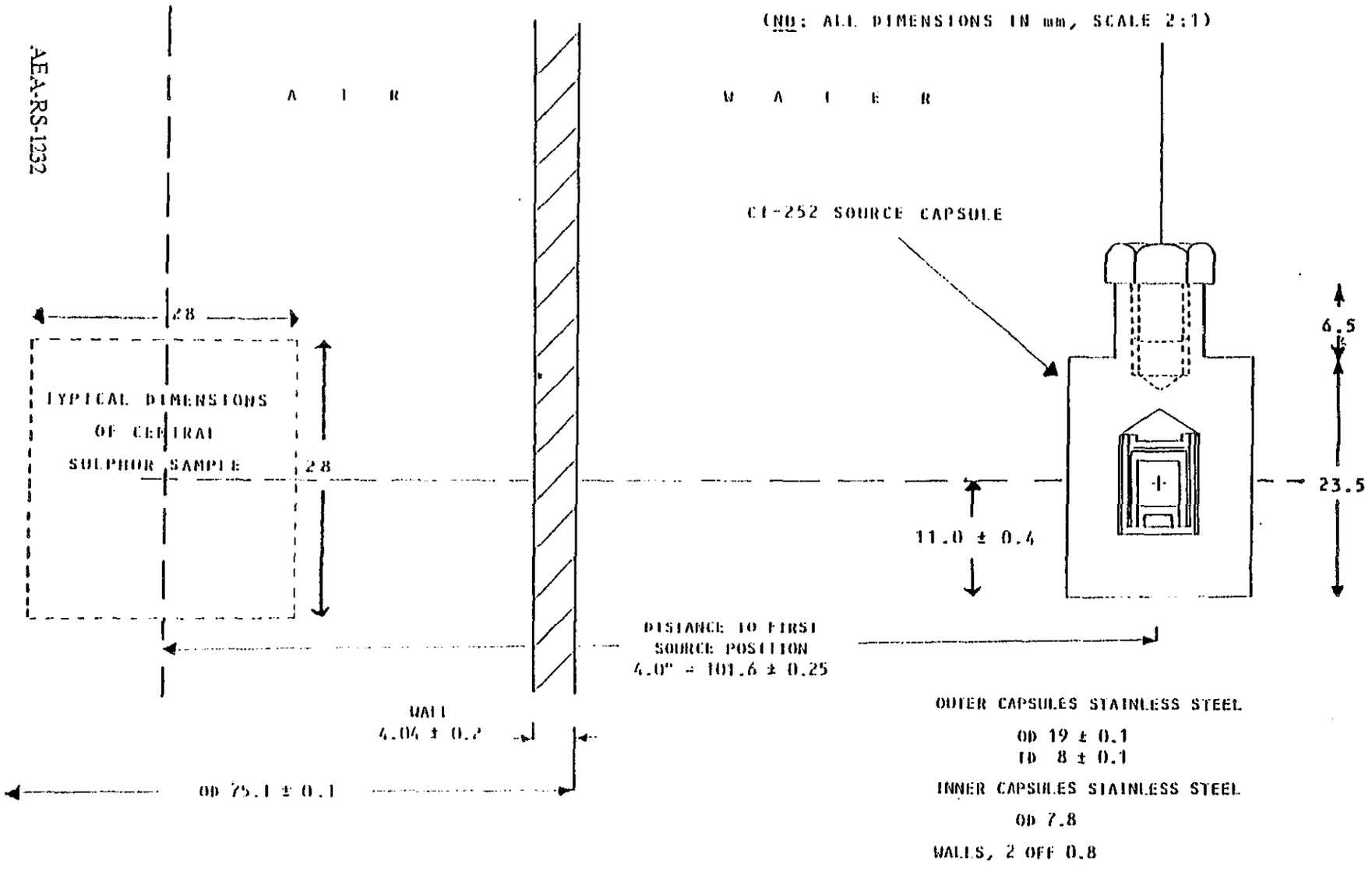

FIGURE 2: DETAIL OF THE WATER BENCHMARK EXPERIMENT

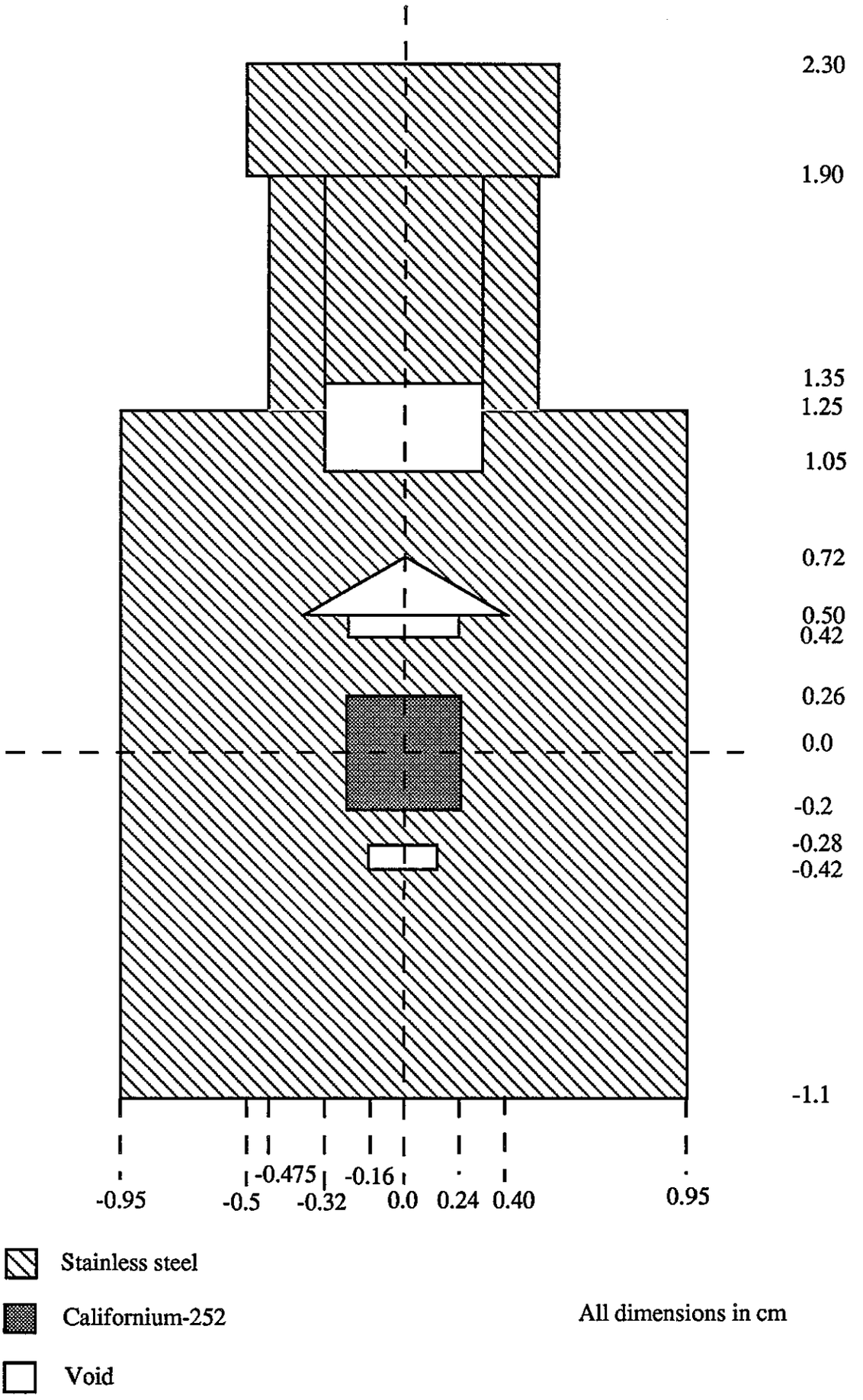

Figure 3. Model of the Source Capsule.

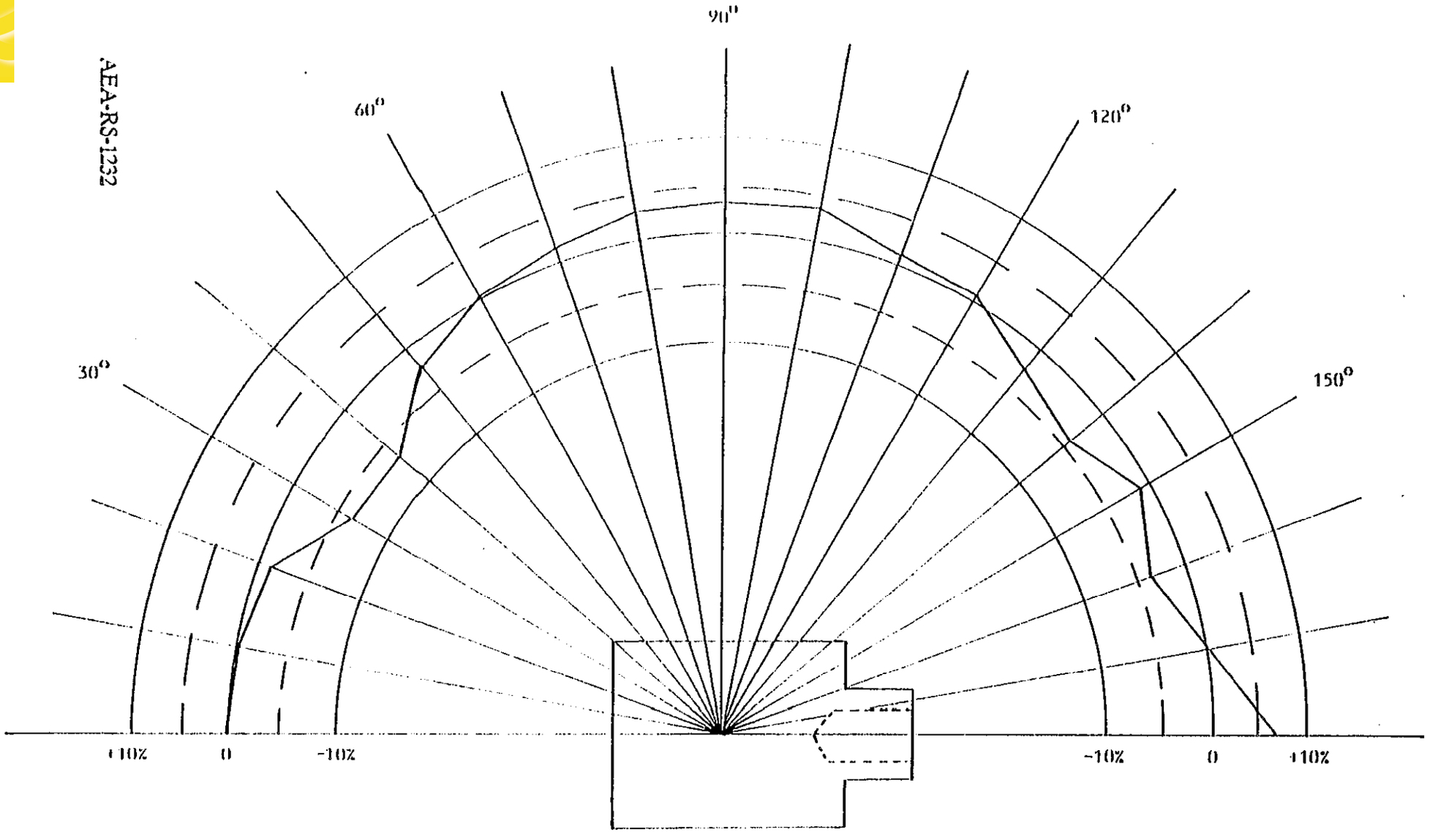

FIGURE 4 : NPL ANISOTROPY MEASUREMENT CF-252 SOURCE NO CVN/20/345

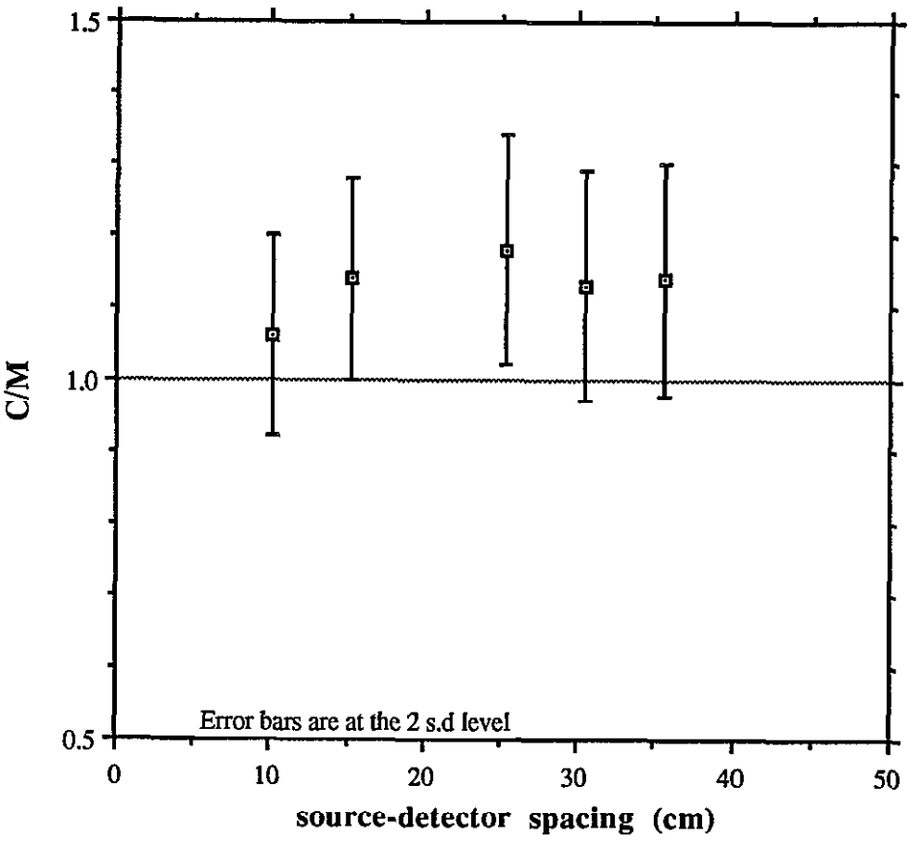

Figure 5. Values of C/M for the S32(n,p)P32 reaction rate in the source plane, for increasing source-detector separation.

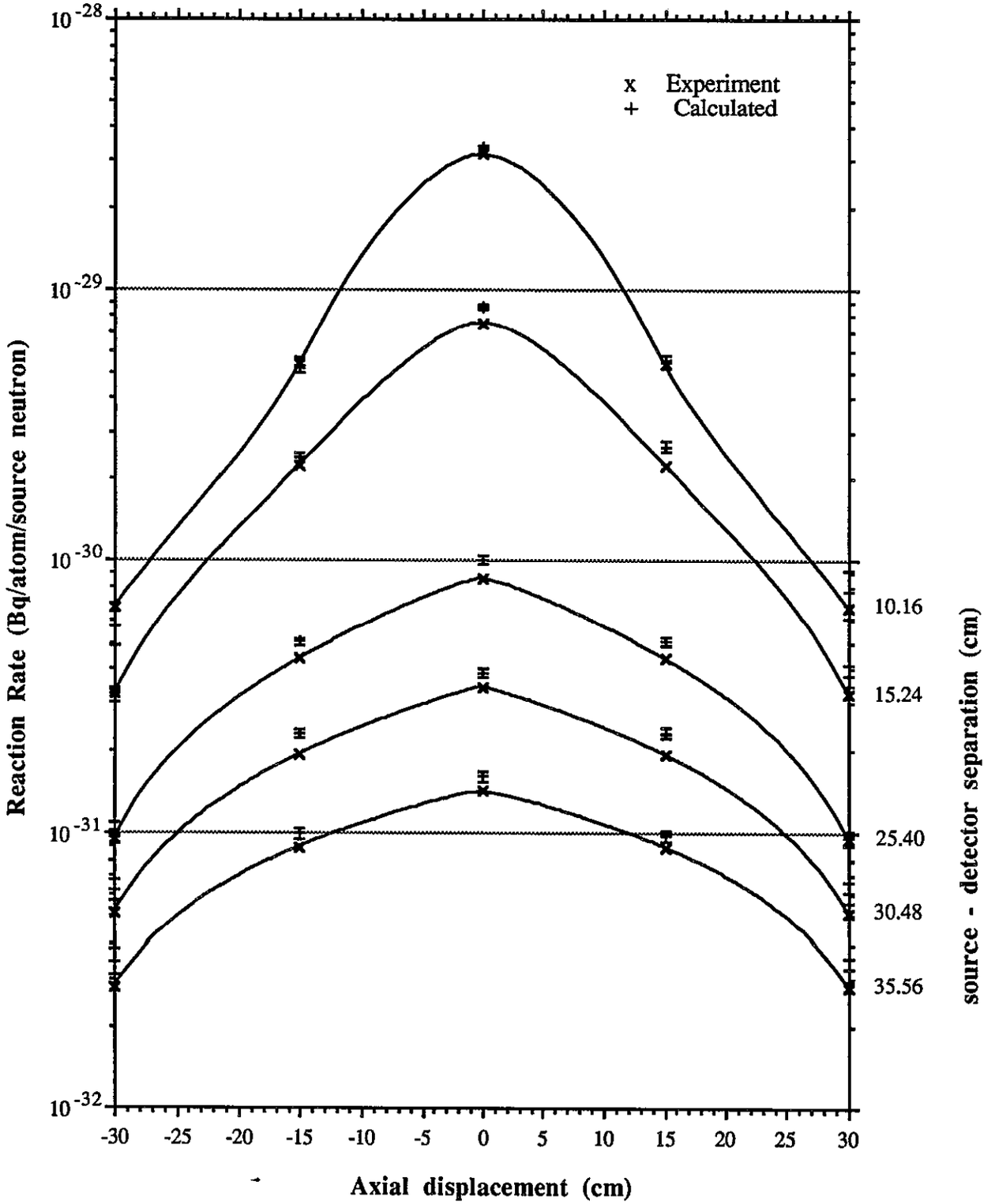

Figure 6. Axial Comparison of S32(n,p)P32 Reaction rates

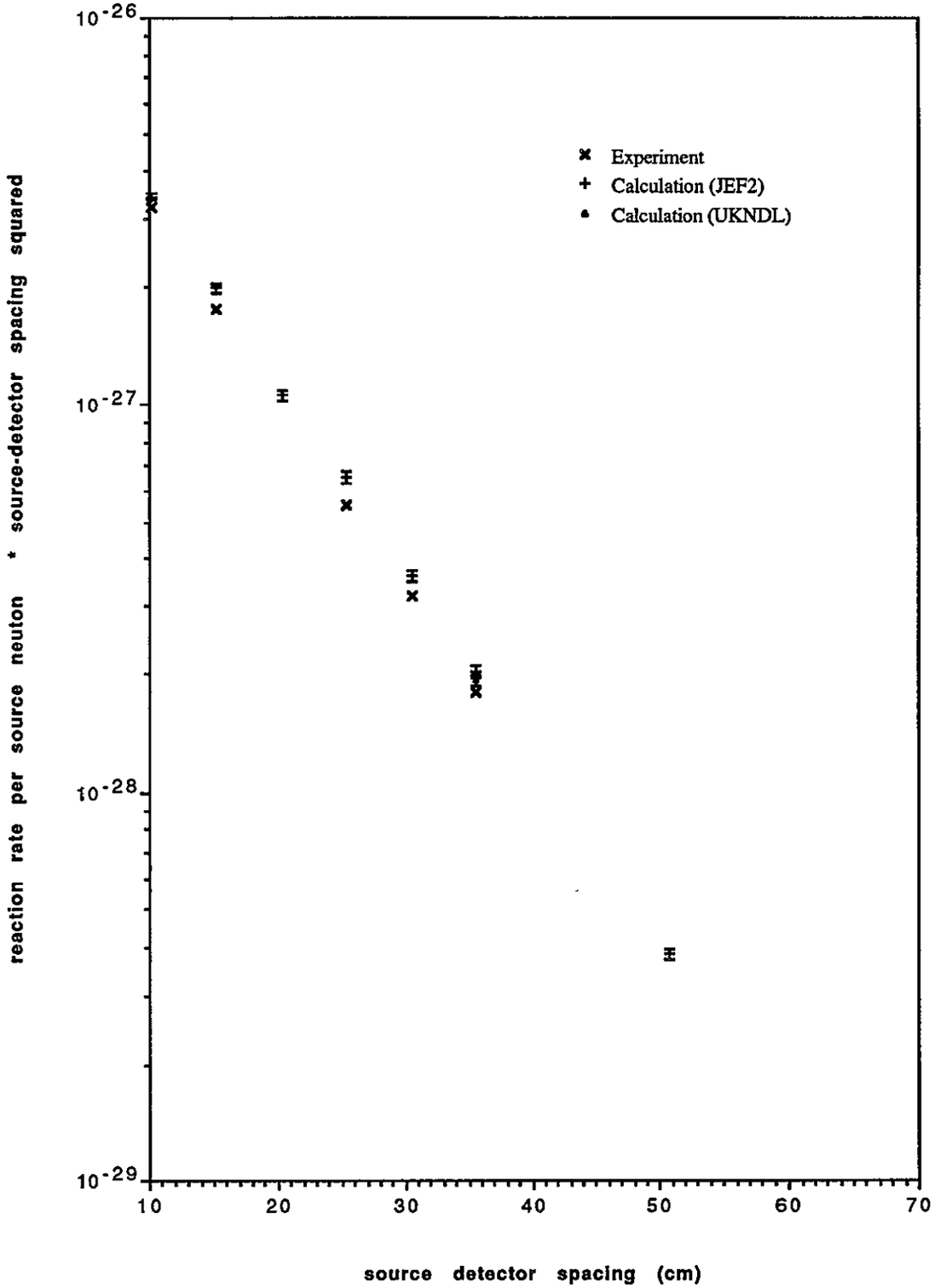

Figure 7. S32(n,p)P32 Reaction rates in the source plane for different source-detector spacings.

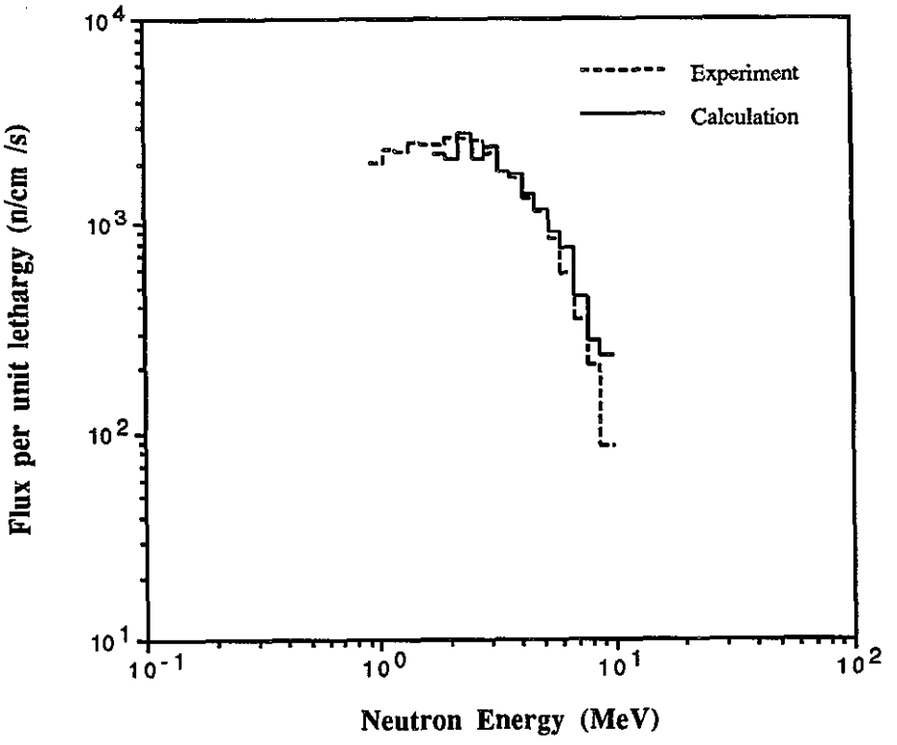

Figure 8. Neutron spectrum at 10.16cm.

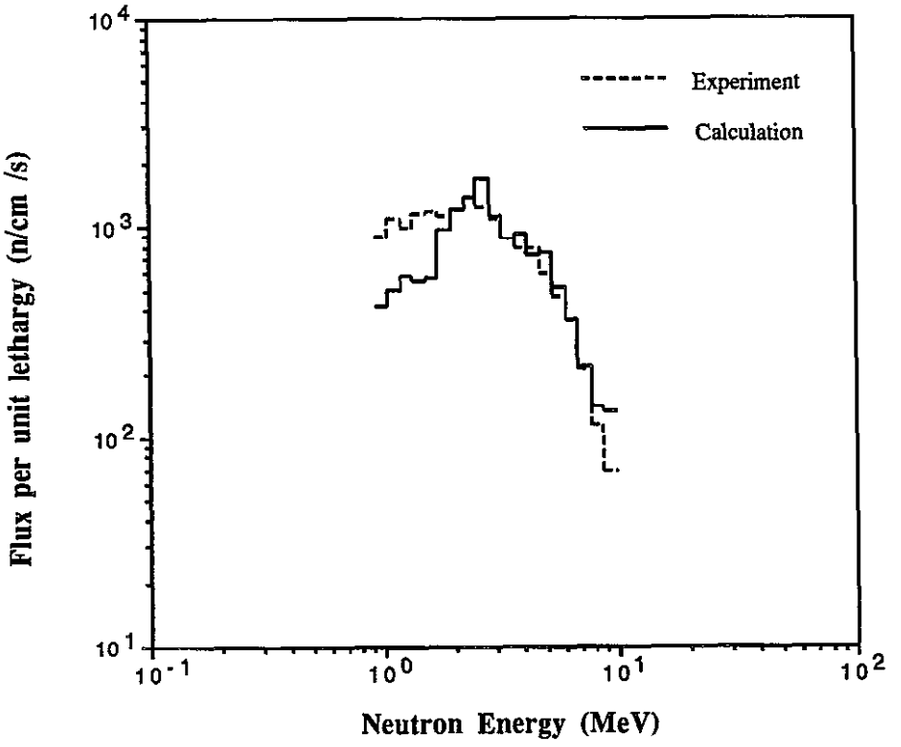

Figure 9. Neutron spectrum at 15.24cm .

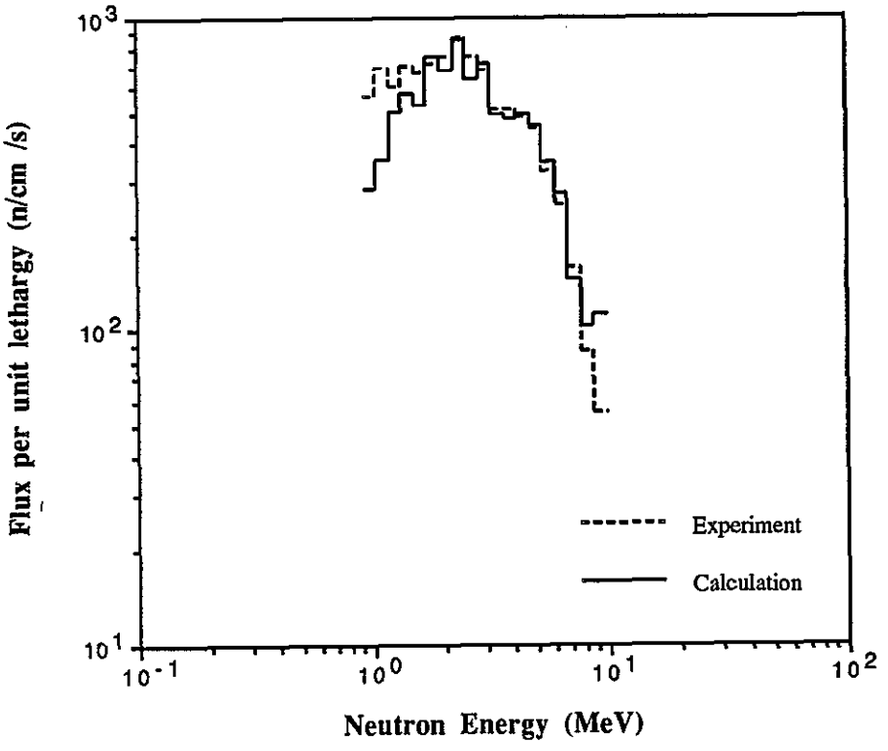

Figure 10. Neutron spectrum at 20.32cm.

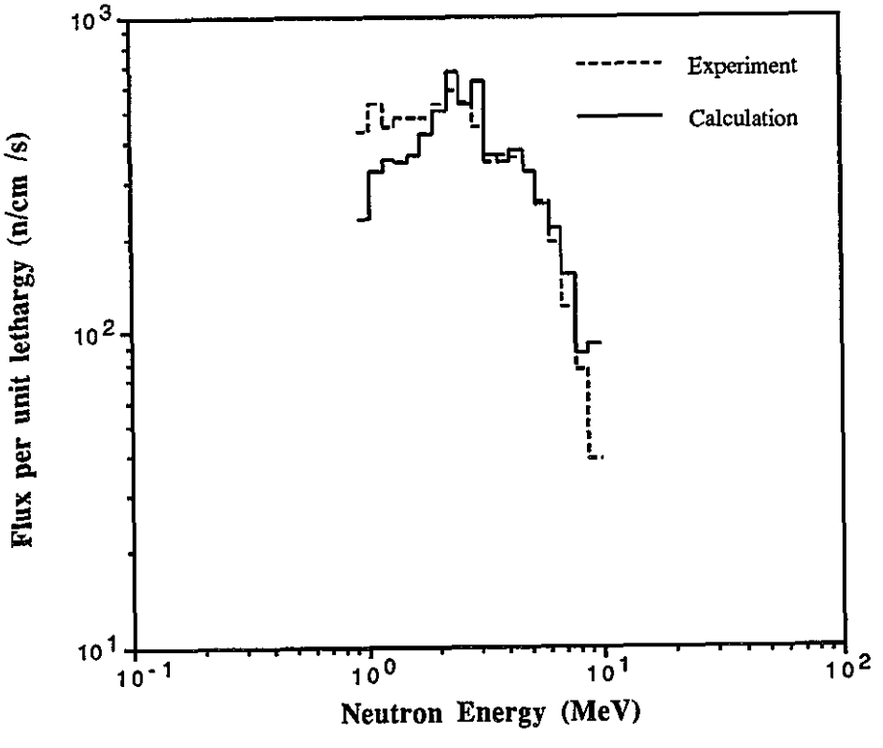

Figure 11. Neutron spectrum at 25.4cm.

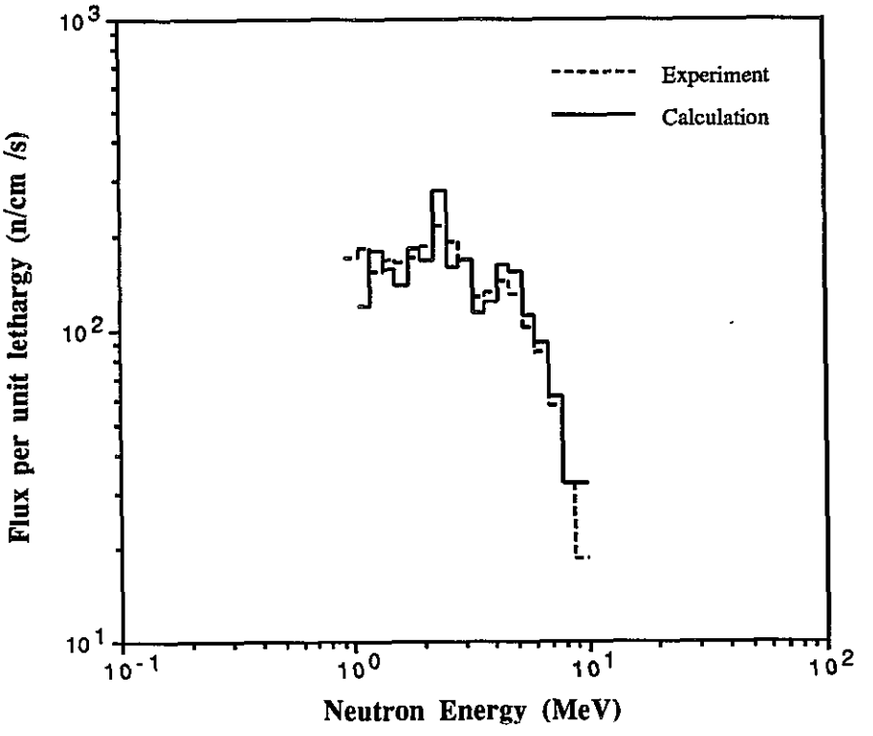

Figure 12. Neutron spectrum at 30.48cm.

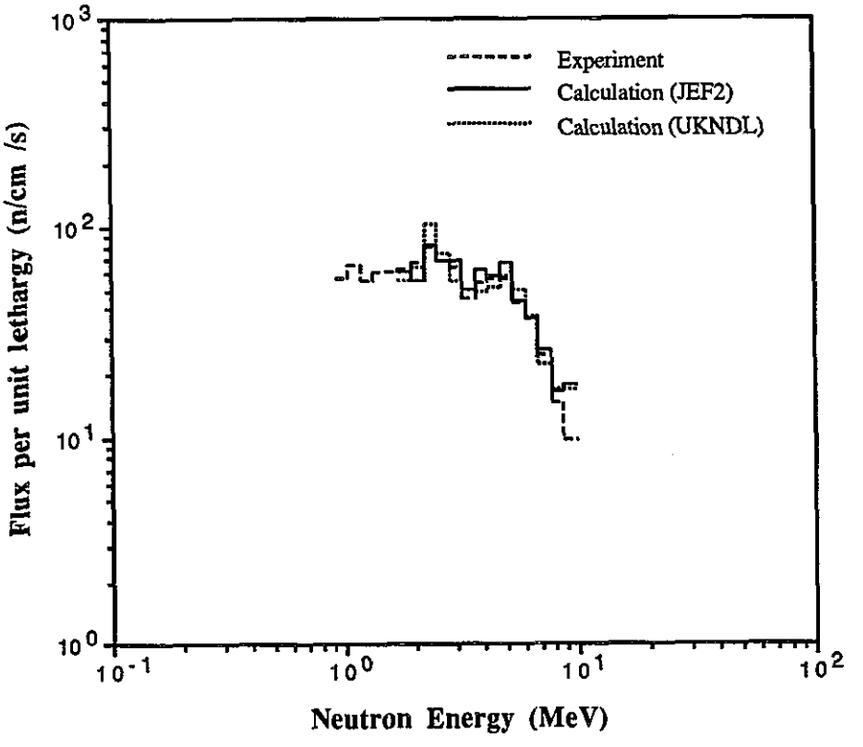

Figure 13. Neutron spectrum at 35.56cm.

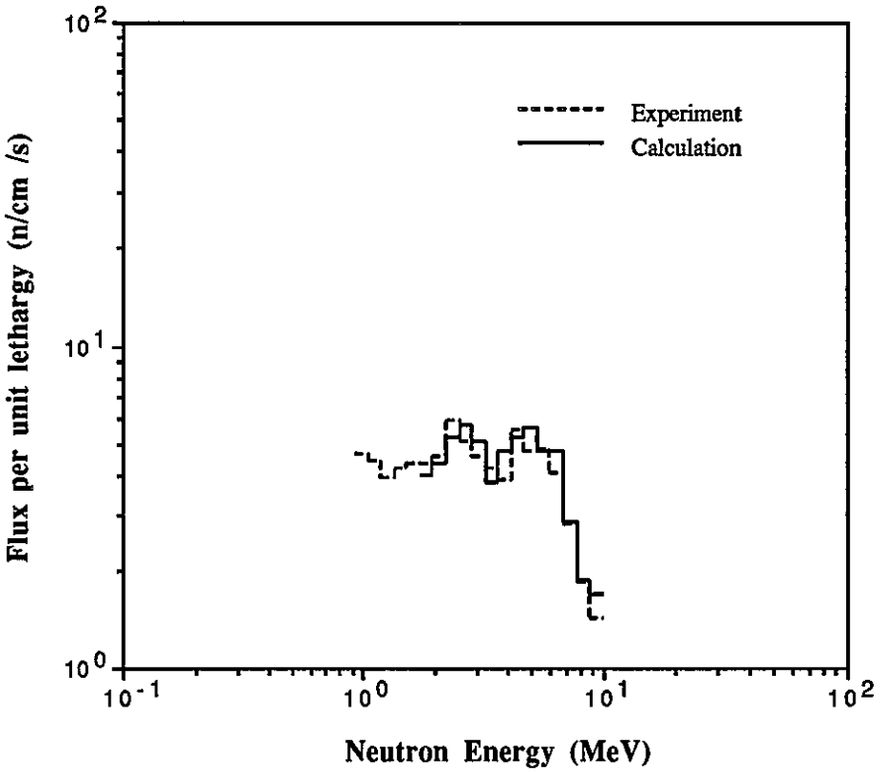

Figure 14. Neutron spectrum at 50.8cm.

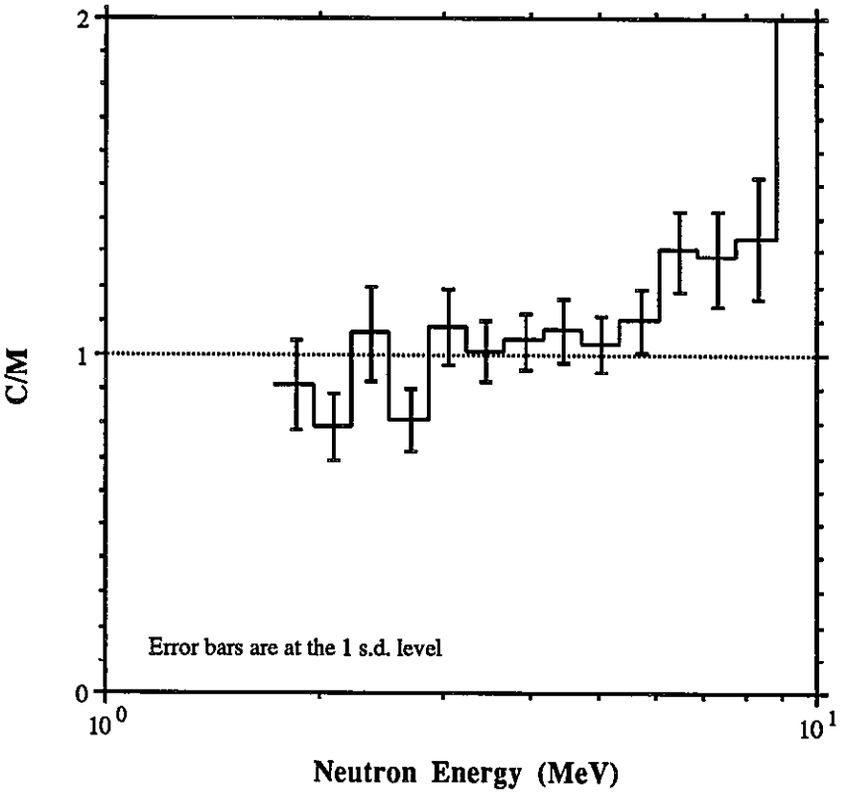

Figure 15. Ratio of Calculated to Measured spectrum at 10.16cm.

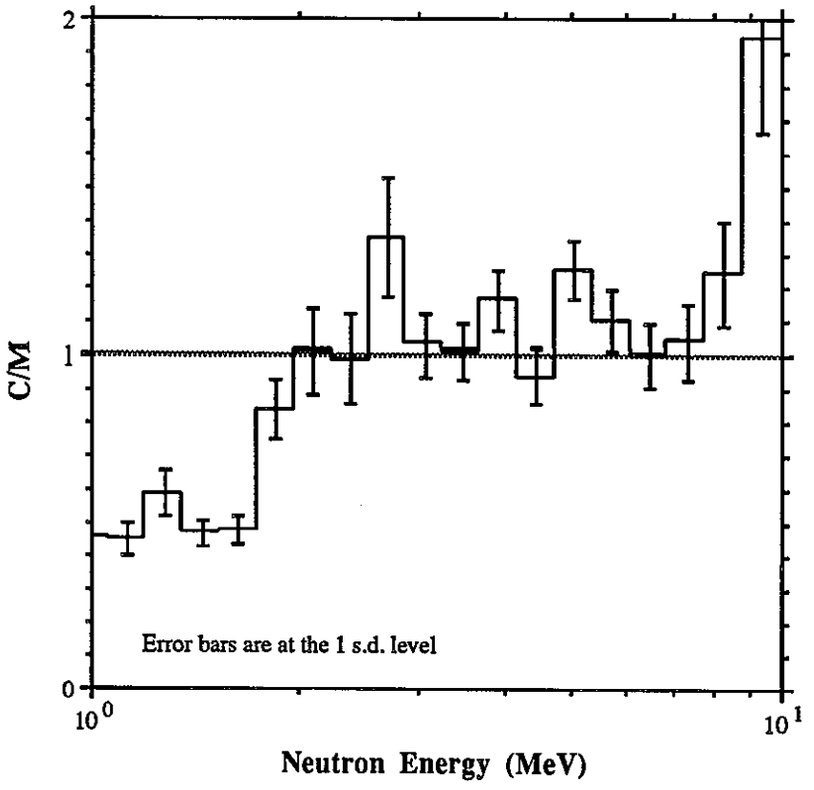

Figure 16. Ratio of calculated to measured spectrum at 15.24cm.

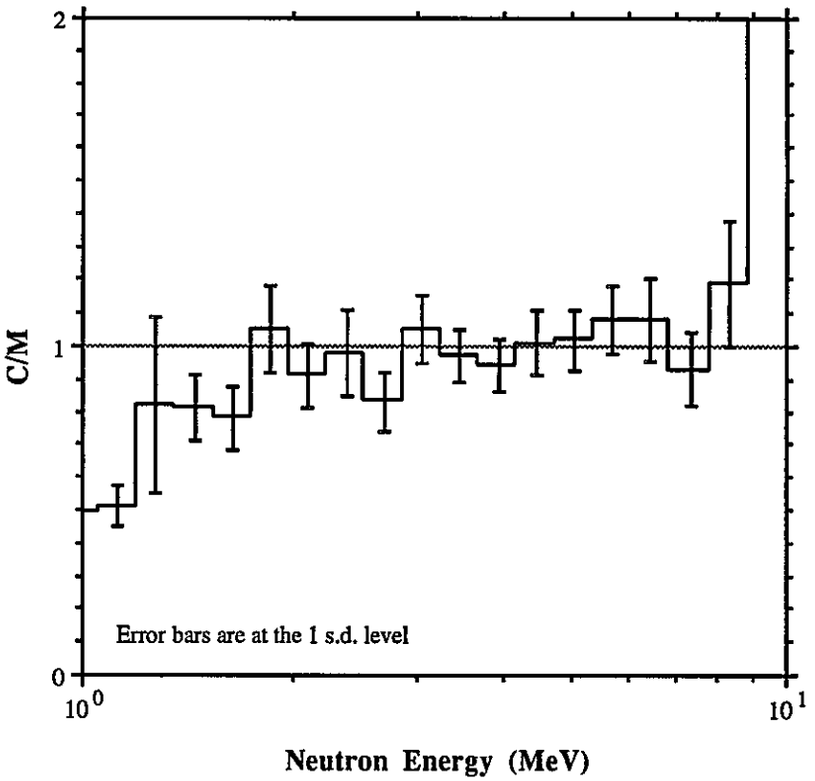

Figure 17. Ratio of calculated to measured spectrum at 20.32cm.

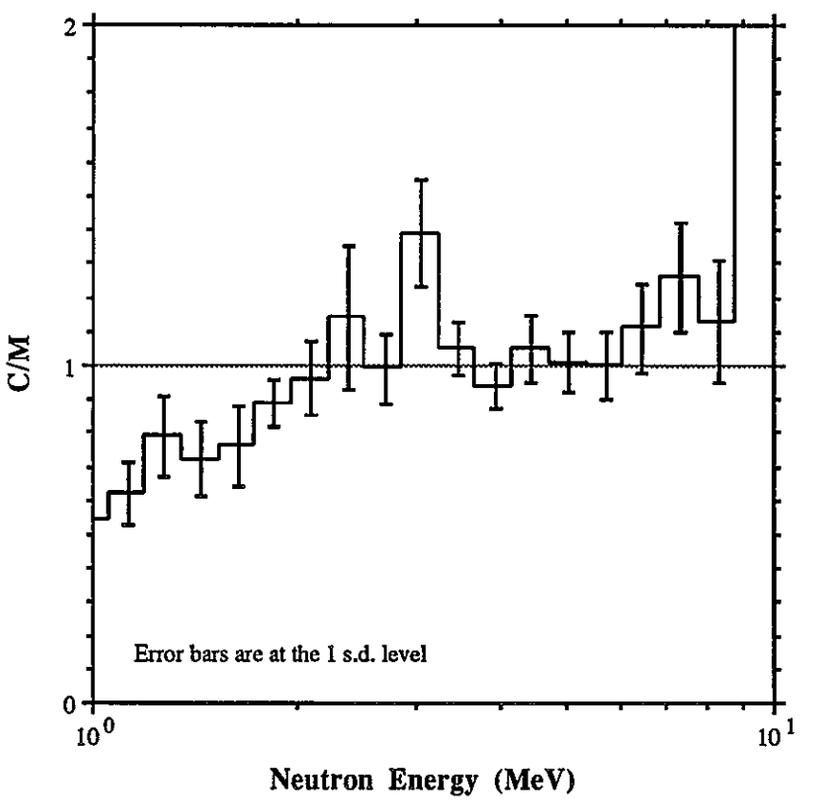

Figure 18. Ratio of calculated to measured spectrum at 25.40cm.

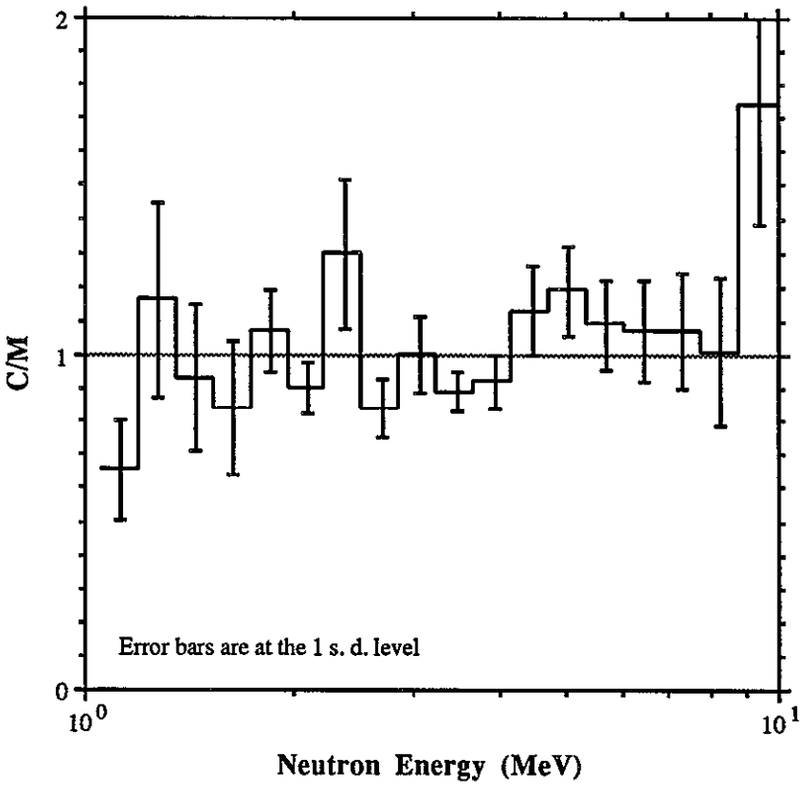

Figure 19. Ratio of calculated to measured spectrum at 30. 48cm.

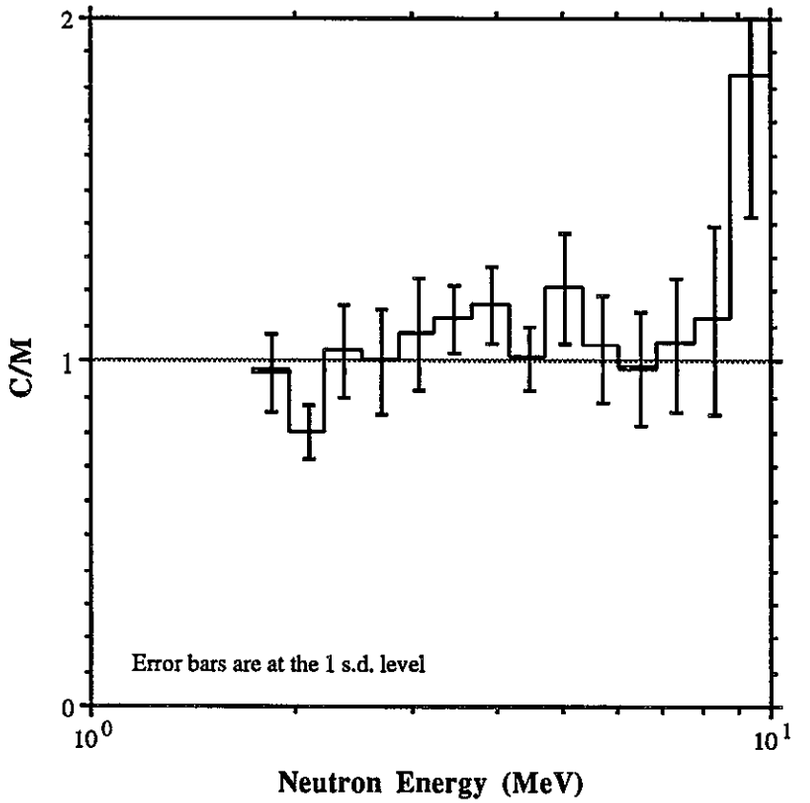

Figure 20. Ratio of calculated to measured spectrum at 35.56cm.

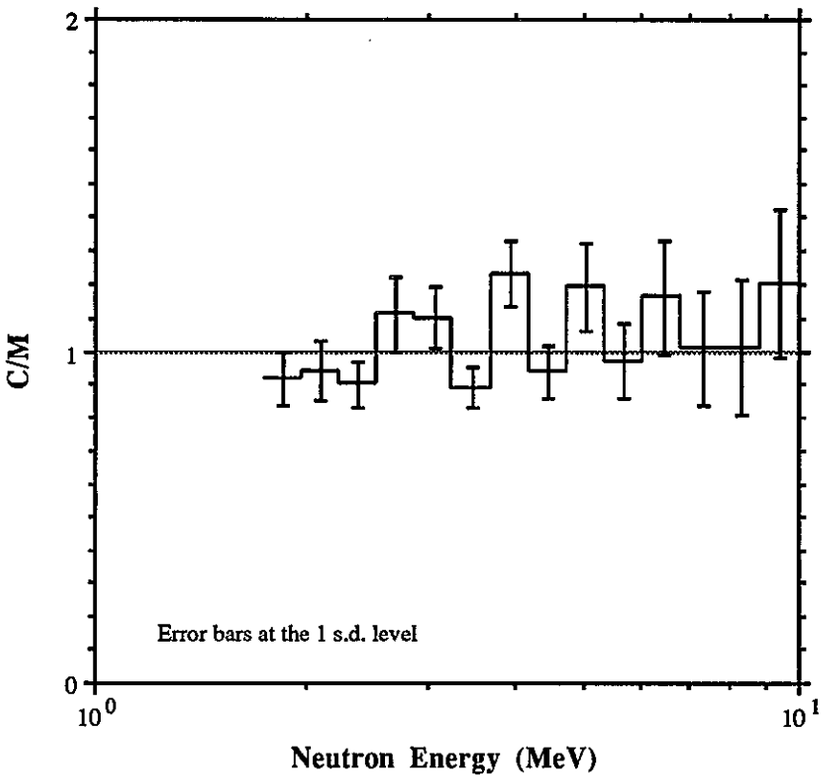

Figure 21. Ratio of calculated to measured spectrum at 50.8cm.